eXPRESS Polymer Letters Vol.11, No.3 (2017) 199–208
Available online at www.expresspolymlett.com
https://doi.org/10.3144/expresspolymlett.2017.21

Modeling polymeric gels: The role of chain flexibility on the structure of physical gels

R. G. Pereyra[1,2*], *M. A. Al-Maadeed*[3], *M. A. Carignano*[4]

[1]Facultad de Matemática, Astronomía y Física, Universidad Nacional de Córdoba, X5000HUA Córdoba, Argentina
[2]IFEG-CONICET, X5016LAE Córdoba, Argentina
[3]Center for Advanced Materials, Qatar University, Doha, Qatar
[4]Qatar Environment and Energy Research Institute, Hamad bin Khalifa University, P.O. Box 5825, Doha, Qatar

Received 29 August 2016; accepted in revised form 3 November 2016

Abstract. Using molecular dynamics simulations and a simple model for chain molecules we study the gel formation under different conditions. The main characteristic of the model is the short attractive range of the non-bonding interaction, which leads to the formation of a single percolated cluster trapped in long lived metastable state that resemble the properties of polymeric physical gels. The gels are formed by imposing a sudden quenching on well equilibrated high temperature conformations. In particular, we investigated the effect of concentration and polymer persistence length on the resulting percolated structures. Using a Monte Carlo approach, we characterize the size of the cavities that develop inside the bulk of the gels. The results show that polymers with higher persistence length produce gel structures with smaller cavities.

Keywords: *modeling and simulation, polymer gels, structural propierties*

1. Introduction

A polymer gel is an entangled network of physically and/or chemically linked polymers immersed in a liquid medium and trapped in a long lived metastable state [1–5]. This so called gel state can be achieved using simple model interactions provided that the range of interaction is very small when compared with the typical size of the interacting particles [6–10]. The physical properties of the gel are intermediate between those of a solid and a liquid and there is considerable interest on them due to their numerous industrial, analytical and domestic applications [11–13]. From a modeling point of view, the understanding of polymeric gels is challenging because of several factors. The fact that the gel state is not a thermodynamic equilibrium imposes a degree of arbitrariness that calls for a compromising answer between what is computationally feasible and what reproduces the known experimental features. The large molecular weight of polymers has to be accounted for by using long enough model chains. This, in turn, opens a number of options for the protocol used to form the systems from initial conditions that are perhaps unrepresentative of realistic situations.

In this study we focus only on physical gels [14–16]. Namely, the interaction between the polymer molecules is reversible as opposed to the formation of chemical links between initially distinguishable molecules. This kind of systems, also referred to as thermoreversible gels, change from polymer solution state to gel state when the temperature changes. There are essentially two kinds of thermoresponsive gels: those presenting a solution-to-gel transition when temperature decreases [17–21] and those having an inverse behavior, for example the PEG-PLGA block

*Corresponding author, e-mail: pereyra@famaf.unc.edu.ar

copolymers [22]. For the first case (solution at high *T* and gel at low *T*), when a temperature quench is applied to a polymer solution, the attractive interactions between the molecules tend to induce a separation into a polymer rich and a polymer poor phases (or into a solid and a very dilute solution). On the other hand, if the cooling is sufficiently fast, the chains form entangled domains that induce a kinetic frustration to the phase separation process. This latter situation eventually reaches a very slow kinetic stage resulting in what we define as a gel.

Gels undergo extraordinarily large volume changes as a reaction to different types of stimuli like changes of temperature, pH and ionic concentration [23–26] and this property is exploited for many applications such as absorbent materials, separation agents, drug delivery systems [27, 28] , polymer dosimetry [29], actuators [30] and sensors [31] among many other. The phenomenon of contraction or dilatation of polymer gels induced by external stimuli can be used to make controllable membranes, as is the case in gel permeation chromatography [32]. Without going to the particular factors that induce the changes of volume, it is clear that the size of the porous in a polymer gel is a determining factor for many practical applications [33, 34].

Understanding the relation between the molecular characteristic of the polymers and solvent type with the structural properties of the resulting gel is a complex task which has not been fully explored. In this sense computer simulations can shed light on this issue providing an important complement to experimental work and analytical theories. There are several computational works where the polymer gel properties have been studied choosing different molecular models and using different simulation techniques [35–38]. Most of them are related with the study of fundamental aspects of network elasticity and of phase transitions in polymeric gels.

Here we study the structure of physical polymer gels modeled by simplified linear chain molecules subject to a strong and short-ranged interaction between the constituent monomers. In particular, we study what is the effect of the polymer concentration and chain flexibility in the structure of the gels and the typical size of the porous after long stabilization. Additionally, we propose a simple Monte Carlo approach to calculate the size of the resulting cavities in the gel.

2. Computational details

The study that we present here is based in molecular dynamics (MD) simulations performed in the NVT ensemble on a cubic cell using periodic boundary conditions and model polymer molecules in an implicit, continuous solvent. The polymer molecules are described using a simple, generic model consisting of a chain of *N* beads of mass *m*. All non-bonded beads interact with a shifted Lennard-Jones potential of the form (Equation (1)):

$$U_{\mathrm{NB}}(r) = 4\varepsilon\left[\left(\frac{\sigma}{r-r_0}\right)^{12} - \left(\frac{\sigma}{r-r_0}\right)^{6}\right] \tag{1}$$

Here, *r* is the distance between beads, ε and σ control the strength and range of the interaction potential, and r_0 is the shifting parameter that controls the size of the particles.This functional form allows for the control of the range of attraction of the interactions and the particle size in an independent manner. For the present case, we have used ε =1 kJ/mol, σ = 0.1 nm and r_0 = 1 nm. This choice was done to ensure a short attractive range for the bead's non-bonded interaction so that the formation of a percolated metastable cluster is achieved upon a sudden reduction of the temperature, as demonstrated in our previous publications for colloidal systems [9, 10].

The connectivity between neighboring beads is maintained using a bonding potential created by combining a finitely extensible nonlinear elastic (FENE) potential [39] and the repulsive part of U_{NB}. Namely, $U_{\mathrm{B}}(\mathrm{r}) = U_{\mathrm{F}}(\mathrm{r}) + U_{\mathrm{R}}(\mathrm{r})$ with (Equations (2) and (3)):

$$U_{\mathrm{F}}(r) = -\frac{1}{2}K_{\mathrm{f}}r_{\mathrm{f}}^2\ln\left[1-\left(\frac{r-r_0}{r_{\mathrm{f}}}\right)^2\right] \tag{2}$$

and

$$U_{\mathrm{R}}(r) = \begin{cases} \infty & \text{for} \quad r \le r_0 \\ U_{\mathrm{NB}}(r) + \varepsilon & \text{for} \quad r_0 < r < r_0 + 2^{1/6}\sigma \\ 0 & \text{for} \quad r_0 + 2^{1/6}\sigma \le r_0 \end{cases} \tag{3}$$

The parameters for Equation (2) are K_{f} = 30 kJ/mol/nm^2 and r_{f} = 1.5 nm. The rigidity of the polymer chains is controlled using a harmonic angular potential $U_{\mathrm{A}}(\theta) = 1/2\cdot K_\theta\cdot(\theta-\pi)^2$, where θ is the angle between two consecutive bonds. By varying the value of K_θ between 0 and 0.01 kJ/mol we obtain a different persistence length for the model polymer as shown below on Table 1.

All the simulations were carried out using the Gromacs package v.4.5.5 [40]. The convention used by

Table 1. Results of cavity size of all simulations of this work. In cases of $K_\theta = 0.001$ and 0.01 for $M = 10$ and $T = 0.083$, there are three numbers inside the cell, corresponding to the three different trajectories

K_θ	ρ	R_M					
		$M = 10$					100
		$T = 0.083$			0.141	0.208	0.083
0.0001	0.2	1.76			2.00	2.91	
	0.1	3.33			3.77	4.98	
	0.02	13.96			17.16	*	
	0.01	26.85			*	*	14.03
0.0003	0.2	1.53					
	0.1	3.10					
	0.02	11.32					
	0.01	22.98					
0.001	0.2	1.44	1.45	1.40	1.62	2.16	
	0.1	2.61	2.49	2.56	3.29	4.00	
	0.02	10.21	9.84	9.45	13.09	13.45	
	0.01	18.08	19.13	17.53	18.92	20.50	9.92
0.003	0.2	1.30					
	0.1	2.28					
	0.02	7.74					
	0.01	12.23					
0.01	0.2	1.17	1.14	1.14	1.34	1.42	
	0.1	2.12	2.04	2.02	2.32	2.65	
	0.02	6.53	6.68	6.59	7.64	9.31	
	0.01	11.27	10.53	11.13	13.31	15.82	6.63

*System does not form a gel and phase separation is observed

Gromacs to define all the interaction parameters is based on real physical units. Nevertheless, as it is customary for studies that aim to find general relations that are independent of particular chemical details we prefer to use reduced units. For that purpose we define the unit of length as r_0 and then the corresponding reduced variable is $r^* = r/r_0$. In other words, all lengths are expressed as their ratio to r_0 and therefore they are dimensionless. All energies are measured in terms of the Lennard-Jones parameter ε, and then the reduced temperature is $T^* = k_B \cdot T/\varepsilon$. Finally, the mass of the beads is used to define the reduced time $t^* = (t/r_0)\sqrt{\varepsilon/m}$. Henceforth we will use exclusively reduced units and, for the sake of clarity, we will omit the asterisks. The reduced parameters for the model are as follow: $\sigma = 0.1$, $K_f = 30$ and $r_f = 1.5$.

The leapfrog algorithm was used for the integration of the dynamics equations, with a time-step 0.001. A spherical cut-off at $r = 7$ was imposed to the non-bonded interactions. The temperature of the system was controlled using a V-rescale thermostat, with time constant of 0.1.

The procedure that we followed to create the gel systems started with a high temperature simulation ($T = 3.33$) in order to reach a randomized configuration. Then, the formation of the gel starts by a sudden quenching to the target temperature. If the concentration is sufficiently high and the target temperature sufficiently low, the system evolves to form a percolated cluster that represents the metastable gel structure. All gel simulations were based on chain molecules having $N = 500$ beads. The majority of the simulated systems contain $M = 10$ macromolecules in the simulation box and in same cases we studied larger systems with $M = 100$ chains. All simulations were extended up to 20 000 times units.

The rigidity of the polymer model is controlled by the angular harmonic parameter K_θ. We carried out simulations with five values of K_θ (0.0001, 0.0003, 0.001, 0.003 and 0.01). The persistence length λ for the model, calculated under good solvent conditions at $T = 0.83$, follows a simple linear relation with the harmonic angular constant. The regression line between λ and K_θ, which has a correlation coefficient of 0.999, yields (Equation (4)):

$$\lambda = 4499K_\theta + 0.8568 \quad (4)$$

Then, it is equivalent to describe the rigidity of the chains by K_θ or λ. We opted to present all the results in terms of K_θ. Our study also include four different values for the polymer concentrations, $\rho = 0.01$, 0.02, 0.1 and 0.2; and three different target temperatures $T = 0.083$, 0.141 and 0.208. For $M = 10$ the four densities are obtained with simulation cells of size $L = 28.0$, 35.5, 60.7 and 76.5. For $M = 100$, the study was performed only for $\rho = 0.02$ with a simulation box of size $L = 130.7$.

3. Results and discussion

In order to understand the model polymers and how they respond to temperature changes we studied the time average squared radius of gyration, R_g^2, of isolated fully flexible ($K_\theta = 0$) chains as a function of the number of beads N. The interaction between non-bonded beads is short-ranged and therefore the transition between good and bad solvent conditions is very abrupt. For large enough T, the chains behave as self avoiding walks with the corresponding Flory exponent $\nu \simeq 0.6$. For $T \leq 0.45$ the squared radius of gyration of the chains sharply decreases. The average equilibrium thermodynamics of the system is well described by direct MD simulations only if the temperature is high enough to overcome the trapping in particular configurations of very low potential

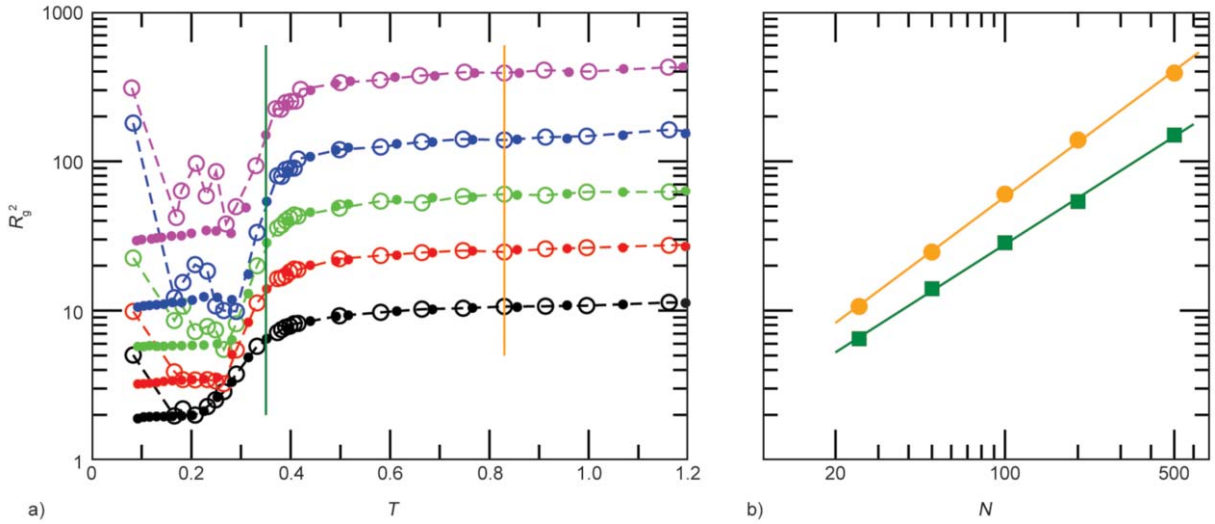

Figure 1. a) Mean square radius of gyration for fully flexible model polymer chains with $N = 25$ (black), 50 (red), 100 (green), 200 (blue) and 500 (magenta) beads. The open symbols connected with dashed lines correspond to results obtained with simple MD simulations, while the filled symbols are obtained from replica exchange MD simulations in a single run spanning all displayed temperatures. b) R_g^2 vs. N for good solvent conditions (orange, $T = 0.83$) and nearly conditions (dark green, $T = 0.35$). The fitted straight lines represent a Flory exponent of 0.604 and 0.517 respectively. The regressions' correlation coefficient are larger than 0.9 in both cases.

energy. Therefore for low temperatures the R_g^2 measured in an individual simulation does not correspond to a real equilibrium quantity but to a particular trapped state. This problem can be easily overcame (for the single chain) by performing a replica exchange MD simulation study. The results are presented in Figure 1 for direct and replica exchange simulations [41]. The transition between the swollen and globular regimes occurs at $0.25 < T < 0.5$. Analysis of the dependency of R_g^2 vs. N reveals that the Θ temperature for the fully flexible model is $\Theta = 0.35$. Therefore, for $T > 0.5$ the system is in the good solvent, high temperature regime. For $T < 0.25$ the system is in the globular, low temperature regime. All simulations that we have performed for the gel systems are at temperatures smaller than 0.21, which are well in the globular region of the isolated chain response and therefore the finite concentration simulations evolve toward an entangled, kinetically trapped, metastable state.

The most straightforward analysis of the gelation process can be done by monitoring the potential energy associated to the non-bonded interactions, U_{NB}, which directly reflects the time evolution of

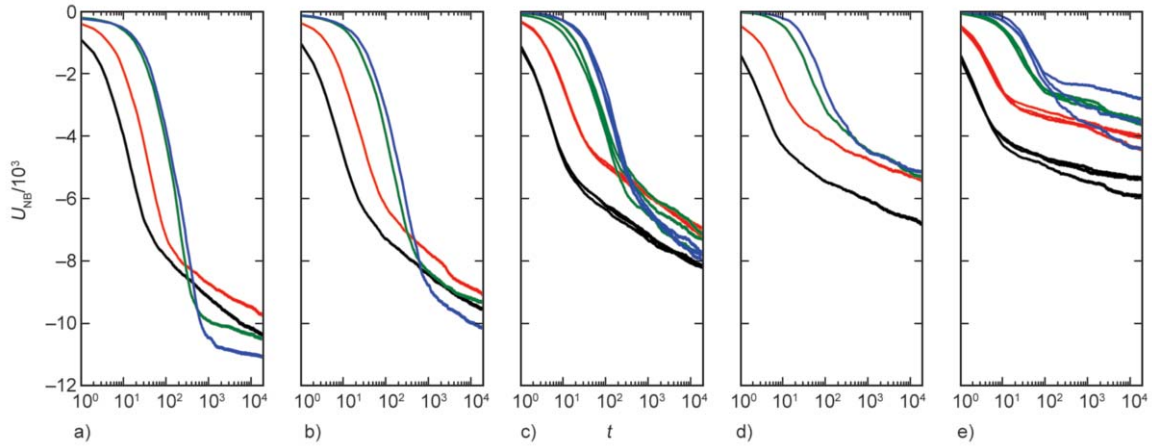

Figure 2. Time evolution of the non-bonding interaction for 36 simulated trajectories at $T = 0.083$, for $N = 500$ and $M = 10$. The panels a), b), c), d) and e) correspond to $K_\theta = 0.0001$, 0.0003, 0.001, 0.003 and 0.01, respectively. The different colors represent different densities $\rho = 0.2$ (black), 0.1 (red), 0.02 (green) and 0.01 (blue). In the panels c) and e) there are three curves for each density corresponding to the trajectories started with three different initial configurations, although in some cases the overlapping of the curves prevent the distinction between the different cases.

the contacts developing between different beads. This is shown on Figure 2 for the four different densities and five different angular potentials. These quenching simulations correspond to a target temperature of 0.083. All curves show the same qualitative pattern that consists of an initial fast decrease representing the formation of physical links between neighboring chains, followed by a slow evolution. After the initial rearrangement of the polymers the dynamics slow down and is reflected by the slope of the potential energy curve that decreases with increasing time. The final value of U_{NB} becomes larger as the harmonic angular constant K_θ increases. Therefore, it could be that the percolated structure obtained with flexible polymer has larger cavities than those of the semi-flexible chains. Namely, the possibility of easy bending allows for the association of many chains in thick threads, therefore the number of threads in the system is small and that results in large free spaces between them. This observation can be quantitatively confirmed by measuring the size of the resulting cavities, as explained below.

For two K_θ values (0.001 and 0.01) we have simulated three trajectories starting from a different initial condition, in order to sample different routes for the gelation process. For the lower value of K_θ we observe a smaller dispersion between the equivalent curves than for the less flexible case, although three curves are perhaps insufficient to draw a solid conclusion. Nevertheless, it is likely that the competition between the non-bonding and bending interactions is more important to determine the system evolution for the molecules with longer persistence length.

A series of snapshots exemplifying a system as it evolves is displayed on Figure 3. The system requires approximately 1000 time units in order to reach a conformation that remains essentially unchanged during the rest of the trajectory. For the represented case, which corresponds to $K_\theta = 0.0003$ and $\rho = 0.02$, one can clearly observe the association between different chains. The conformation reached at the end of the simulation runs, i.e. for $t = 20\,000$, for all the different K_θ and for $\rho = 0.01$ are represented in Figure 4. In these snapshots it is possible to appreciate the qualitative difference emerging as the chains become less flexible. The polymer network covers more uniformly the space for the higher values of K_θ leaving a gel with smaller cavities.

The size of the cavities can be determined by a Monte Carlo procedure based on moving a test sphere in the final configuration of each simulation. The method consists of the following steps:

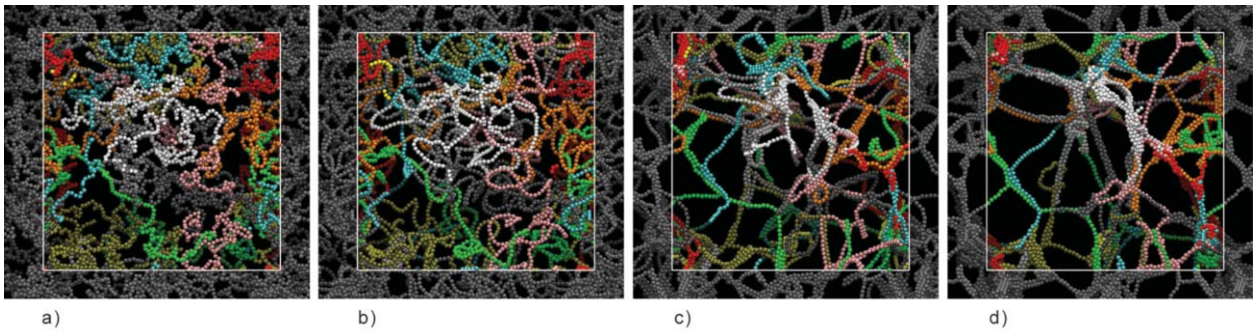

Figure 3. Snapshots corresponding to $N = 500$, $M = 10$, $T = 0.083$ and different times during the simulation corresponding to $K_\theta = 0.0003$ and $\rho = 0.02$. From a) to d): $t = 2$, $t = 20$,$t = 200$ and $t = 2000$. The evolution after the last frame is minimal. The simulation box is represented by the thin white square that frames the individual polymer chains that are distinguished by different colors. A partial view of the image system is represented displaying the polymers in gray.

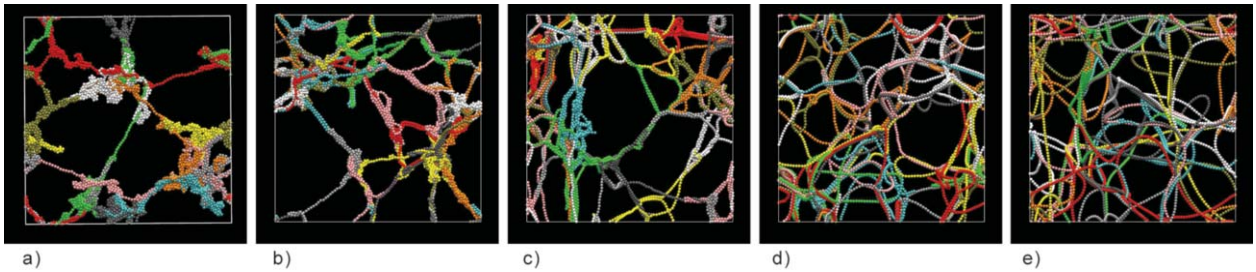

Figure 4. Final configurations corresponding to $K_\theta = 0.0001$, 0.0003, 0.001, 0.003 and 0.01 (a) to e)). Different chains are represented in different colors. The density is $\rho = 0.01$ and the target temperature $T = 0.083$.

1. Define the radius R of the test sphere.
2. Select a randomly chosen trial initial position for the test sphere in the simulation box. Check the overlap of the sphere with the gel, using a critical distance $R + r_0/2 + \sigma$. Note that $r_0/2 + \sigma$ is an approximation for the bead's radius. In case of overlap, select a new position and check again for overlap. Continue until a position with no overlap is obtained. The selected coordinates are $\mathbf{r}_1 = (x_1, y_1, z_1)$. Set $i = 1$.
3. Generate a random displacement $\boldsymbol{\delta} = (\delta x, \delta y, \delta z)$ and test $\mathbf{r}^t = \mathbf{r}_i + \boldsymbol{\delta}$ for overlap. If there is no overlap: define $\mathbf{r}_{i+1} = \mathbf{r}^t$ and $i = i + 1$. If there is overlap: define $\mathbf{r}_{i+1} = \mathbf{r}_i$ and $i = i + 1$.
4. Repeat step 3.

This procedure generates a quasi diffusive process for the test sphere. Generating many initial trial positions the method is able to average the whole structure of the system. By plotting the mean square displacement vs. the Monte Carlo step i we can compute an average effective diffusion constant D that decreases in value as the radius R of the test sphere is increased. For all the final configurations we applied this method using 1000 initial positions, and evolved each one of them for 50 000 steps. In Figure 5 we show D as a function of R for all the simulated systems. In order to determine a quantitative value for the largest size R_M of the cavities we extrapolate the final portion of the curves to determine the intersection with the R axis ($D = 0$). The results are summarized in Table 1 and plotted in Figure 6 using a double logarithmic scale. The dependency of R_M with the polymer concentration and angular rigidity constant can be fitted and is very well represented by the Equation (5):

$$\ln R_M = -0.1427 \cdot \ln K_\theta - 0.8264 \cdot \ln\rho - 1.9527 \qquad (5)$$

Equation (5) shows that increasing the chain bending constant the maximum cavity size decreases following a weak power law. The relation with the polymer concentration is also a power law, but with a stronger dependency.

We continue our analysis by studying the effect of a different target temperature, in particular increasing the temperature closer to 0.25, the upper bound of the globular regime (see Figure 1). These new cases include $T = 0.141$ and 0.208, $K_\theta = 0.0001$, 0.001 and 0.01 and all the previously studied densities. In some cases, which correspond to the most flexible chains with $K_\theta = 0.0001$, we observed that resulting

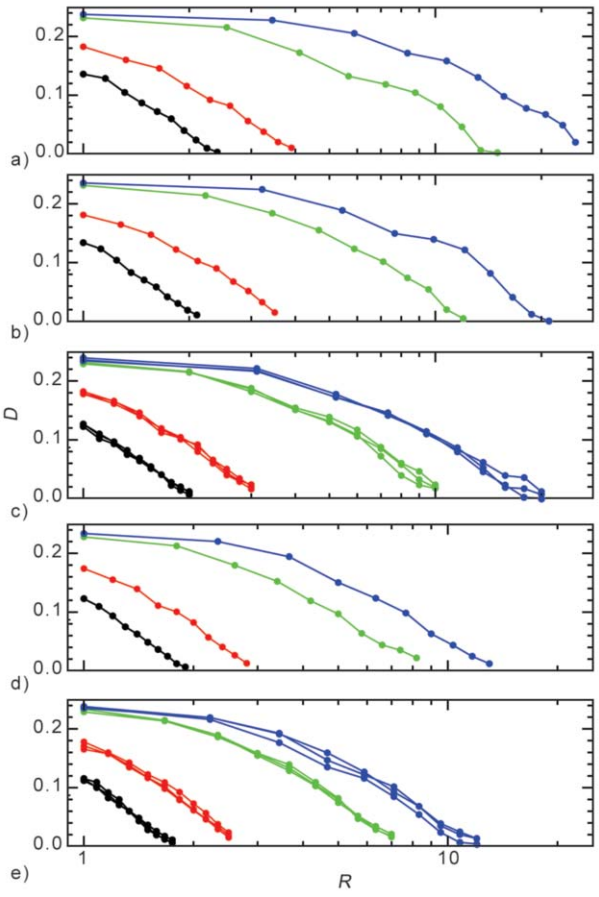

Figure 5. D as a function of R (see the explanation in the text). Each panel corresponds to different rigidities, $K_\theta = 0.0001$ (a), 0.0003 (b), 0.001 (c), 0.003 (d) and 0.01 (e). Each color corresponds to different densities, $\rho = 0.2$ (black), 0.1 (red), 0.02 (green) and 0.01 (blue).

structure obtained after the simulation has lost the connectivity in one Cartesian direction, implying the triggering of a phase separation process that would prevent the formation of the gel. All these anomalous cases are noted with an asterisk in Table 1. A simple visual inspection of the remaining cases that do show the formation of a gel reveals that the size of the cavities slightly increases with increasing target temperature. The larger cavity size for warmer temperature can be explained for the fact that the polymers are allowed to flow to get more links until the kinetic frustration occurs, resulting in a more porous structure. Correspondingly, the potential energy reached at the end of the trajectory is smaller for the higher temperature cases. The quantitative values for the resulting cavity size R_M is included in fourth and fifth columns of Table 1.

It could be argued, by comparing the size of the simulation box with that of the constituent polymer

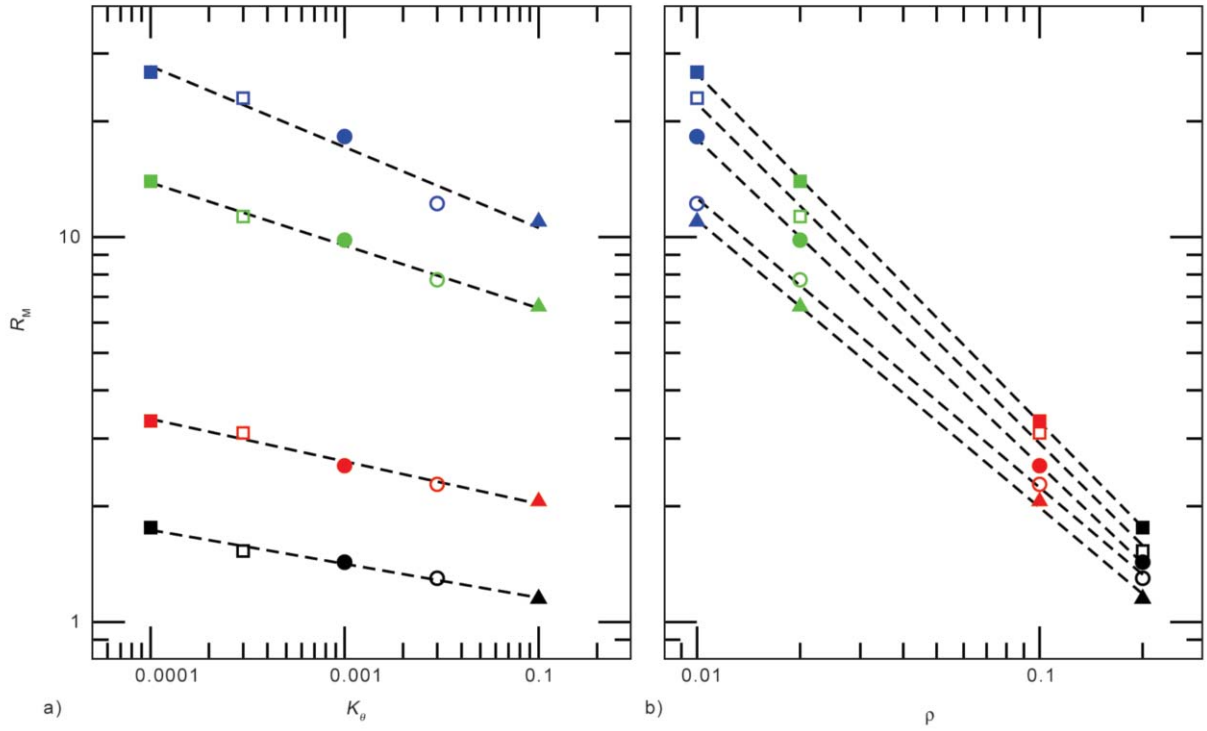

Figure 6. Cavity size vs. system density and rigidity parameter. a) R_M vs K_θ. b) R_M vs ρ. Different color of the symbols correspond to different values of ρ (black: 0.2, red: 0.1, green: 0.02 and blue: 0.01). Different symbols correspond to different values of K_θ (solid square: 0.0001, open square: 0.0003, solid circle: 0.001, open circle: 0.003 and triangle up: 0.01). For the cases $K_\theta = 0.001$ and 0.01 the point showed is the average of R_M of the three trajectories. The segmented straight lines are result of a least square fitting of data.

chains, that there could be an important effect of the size of the simulation cell in the structure of the gels. To investigate this issue, we have carried out extra simulation runs with a system ten times larger than the previous ones. Namely, in these new simulations we represent the system using $M = 100$ polymer chains of $N = 500$ monomers each. We limit this study to only three representative cases with $K_\theta = 0.0001$, 0.001 and 0.01 with $\rho = 0.02$ and $T = 0.083$. In Figure 7 we show the final conformations of these three new cases along with previous corresponding results obtained with the smaller simulation cell. The similitude between the small and large system can be clearly appreciated. Moreover, the quantitative cavity size analysis included in Table 1 confirms that the small system is indeed a good representation that captures sufficiently well the conformational complexity of the polymeric gels.

4. Conclusions

In summary, we have performed a molecular dynamics simulation study of the gelation process starting from a hight temperature polymer solution. We studied the effect of polymer density, persistence length of the individual chains and quenching temperature. We also investigated the appropriateness of our simulation system by performing a few test cases using much larger simulation cells. We have characterized the gel porosity using a single parameter and we have investigated its dependency with the three model parameters. The inverse relation of the cavity size R_M with the density ρ is expected assuming a uniform expansion of the system. The exact relation that we found is a power law dependence $R_M \sim \rho^{-0.83}$. The dependence of R_M with the chain rigidity can be rationalized in terms of the difficulty for the polymers to bend in order to make bundles as K_θ increases. This results in a net effect of the polymer covering the space in a more homogeneous way as the rigidity increases, and consequently leaving an intricate tunnel network. In order to achieve a more homogeneous space covering with the same number of chains, it is necessary to have less links between the different molecules. Nevertheless, this effect follows a weak power law $R_M \sim K_\theta^{-0.14}$. The quenching temperature also affects the size of the resulting structure by inducing larger pores for higher temperatures, provided that the system does not start a phase separation

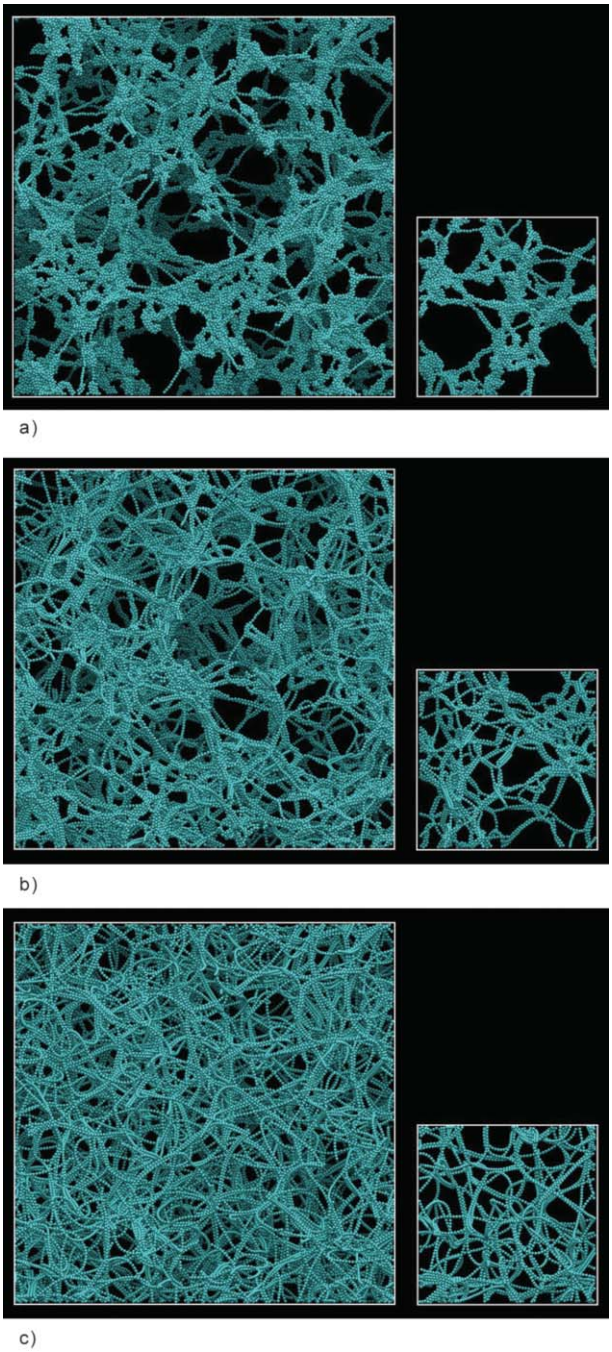

Figure 7. Final configurations corresponding to $K_0 = 0.0001$, 0.001, 0.01 (a) to c)) of the system with $M = 100$ (left) and $M = 10$ chains. The density is $\rho = 0.02$ and the temperature $T = 0.083$.

process. As stated in the Introduction, the characterization of the porosity in gels is important for many applications. This paper is a first step in our long term goal of having a comprehensive picture relating polymer properties and the resulting gel structure.

Acknowledgements

This work was funded by the Qatar National Research Fund, under NPRP grant 6-282-2-119.

References

[1] Flory P. J.: Introductory lecture. Faraday Discussions of the Chemical Society, **57**, 7–18 (1974). https://doi.org/10.1039/DC9745700007

[2] DeRossi D., Kajiwara K., Osada Y., Yamauchi A.: Polymer gels: Fundamentals and biomedical applications. Plenum Press, New York (1991).

[3] Terech P., Weiss, R. G.: Low molecular mass gelators of organic liquids and the properties of their gels. Chemical Reviews, **97**, 3133–3160 (1997). https://doi.org/10.1021/cr9700282

[4] Osada Y., Khokhlov A. R.: Polymer gels and networks. Marcel Dekker, New York (2002).

[5] Dietsch H., Malik V., Reufer M., Dagallier C., Shalkevich A., Saric M., Gibaud T., Cardinaux F., Scheffold F., Stradner A., Schurtenberger P.: Soft nanotechnology from colloid physics to nanostructured functional materials. Chimia International Journal for Chemistry, **62**, 805–814 (2008). https://doi.org/10.2533/chimia.2008.805

[6] Hasegawa M.: Variational perturbation calculations for the phase diagram of systems with short-ranged interactions. Journal of Chemical Physics, **108**, 208–217 (1998). https://doi.org/10.1063/1.475392

[7] Teece L. J., Faers M. A., Bartlett P.: Ageing and collapse in gels with long-range attractions. Soft Matter, **7**, 1341–1351 (2011). https://doi.org/10.1039/C0SM00626B

[8] Bartlett P., Teece L. J., Faers M. A.: Sudden collapse of a colloidal gel. Physical Review E, **85**, 021404/1–021404/13 (2012). https://doi.org/10.1103/PhysRevE.85.021404

[9] Santos P. H. S., Campanella O. H., Carignano M. A.: Brownian dynamics study of gel-forming colloidal particles. Journal of Physical Chemistry B, **114**, 13052–13058 (2010). https://doi.org/10.1021/jp105711y

[10] Santos P. H. S., Campanella O. H., Carignano M. A.: Effective attractive range and viscoelasticity of colloidal gels. Soft Matter, **9**, 709–714 (2013). https://doi.org/10.1039/C2SM26585K

[11] Ross-Murphy S. B.: Rheological characterization of polymer gels and networks. Polymer Gels and Networks, **2**, 229–237 (1994). https://doi.org/10.1016/0966-7822(94)90007-8

[12] Panyukov S., Rabin Y.: Statistical physics of polymer gels. Physics Reports, **269**, 1–131 (1996). https://doi.org/10.1016/0370-1573(95)00068-2

[13] AlMaadeed M. A., Ouederni M., Khanam P. N.: Effect of chain structure on the properties of glass fibre/polyethylene composites. Materials and Design, **47**, 725–730 (2013). https://doi.org/10.1016/j.matdes.2012.11.063

[14] Schupper N., Rabin Y., Rosenbluh M.: Multiple stages in the aging of a physical polymer gel. Macromolecules, **41**, 3983–3994 (2008). https://doi.org/10.1021/ma702613j

[15] An Y., Solis F. J., Jiang H.: A thermodynamic model of physical gels. Journal of the Mechanics and Physics of Solids, **58**, 2083–2099 (2010). https://doi.org/10.1016/j.jmps.2010.09.002

[16] Dahan E., Sundararajan P. R.: Thermoreversible physical gels of poly(dimethylsiloxane) without cross-links or functionalization. Langmuir, **29**, 8452–8458 (2013). https://doi.org/10.1021/la401521m

[17] Semenov A. N., Rubinstein M.: Thermoreversible gelation in solutions of associative polymers. 1. Statics. Macromolecules, **31**, 1373–1385 (1998). https://doi.org/10.1021/ma970616h

[18] Rubinstein M., Dobrynin A. V.: Associations leading to formation of reversible networks and gels. Current Opinion in Colloid and Interface Science, **4**, 83–87 (1999). https://doi.org/10.1016/S1359-0294(99)00013-8

[19] Tosh S. M., Marangoni A. G.: Determination of the maximum gelation temperature in gelatin gels. Applied Physics Letters, **84**, 4242–4244 (2004). https://doi.org/10.1063/1.1756210

[20] Fujigaya T., Jiang D-L., Aida T.: Spin-crossover physical gels: A quick thermoreversible response assisted by dynamic self-organization. Chemistry: An Asian Journal, **2**, 106–113 (2007). https://doi.org/10.1002/asia.200600371

[21] Peak C. W., Wilker J. J., Schmidt G.: A review on tough and sticky hydrogels. Colloid and Polymer Science, **291**, 2031–2047 (2013). https://doi.org/10.1007/s00396-013-3021-y

[22] Zhang K., Tang X., Zhang J., Lu W., Lin X., Zhang Y., Tian B., Yang H., He H.: PEG–PLGA copolymers: Their structure and structure-influenced drug delivery applications. Journal of Controlled Release, **183**, 77–86 (2014). https://doi.org/10.1016/j.jconrel.2014.03.026

[23] Osada Y., Gong J-P.: Soft and wet materials: Polymer gels. Advanced Materials, **10**, 827–837 (1998). https://doi.org/10.1002/(SICI)1521-4095(199808)10:11<827::AID-ADMA827>3.0.CO;2-L

[24] Segarra-Maset M. D., Nebot V. J., Miravet J. F., Escuder B.: Control of molecular gelation by chemical stimuli. Chemical Society Reviews, **42**, 7086–7098 (2013). https://doi.org/10.1039/C2CS35436E

[25] Hoffman A. S.: Stimuli-responsive polymers: Biomedical applications and challenges for clinical translation. Advanced Drug Delivery Reviews, **65**, 10–16 (2013). https://doi.org/10.1016/j.addr.2012.11.004

[26] Mrlík M., Leadenham S., AlMaadeed M. A., Erturk A.: Figure of merit comparison of PP-based electret and PVDF-based piezoelectric polymer energy harvesters. Proceeding SPIE 9799, Active and Passive Smart Structures and Integrated Systems, **2016**, 979923/1–979923/8 (2016). https://doi.org/10.1117/12.2222283

[27] Bajpai A. K., Shukla S. K., Bhanu S., Kankane S.: Responsive polymers in controlled drug delivery. Progress in Polymer Science, **33**, 1088–1118 (2008). https://doi.org/10.1016/j.progpolymsci.2008.07.005

[28] Escobar-Chavez J. J., Merino-Sanjuán V., López-Cervantes M., Urban-Morlan Z., Piñón-Segundo E., Quintanar-Guerrero D., Ganem-Quintanar A.: The tape-stripping technique as a method for drug quantification in skin. Journal of Pharmacy and Pharmaceutical Sciences, **11**, 104–130 (2008). https://doi.org/10.18433/J3201Z

[29] Baldock C., De Deene Y., Doran S., Ibbott G., Jirasek A., Lepage M., McAuley K. B., Oldham M., Schreiner L. J.: Polymer gel dosimetry. Physics in Medicine and Biology, **55**, R1–R63 (2010). https://doi.org/10.1088/0031-9155/55/5/R01

[30] Maeda S., Hara Y., Yoshida R., Hashimoto S.: Active polymer gel actuators. International Journal of Molecular Sciences, **11**, 52–66 (2010). https://doi.org/10.3390/ijms11010052

[31] Lev O., Tsionsky M., Rabinovich L., Glezer V., Sampath S., Pankratov I., Gun J.: Organically modified sol-gel sensors. Analytical Chemistry, **67**, 22A–30A (1995). https://doi.org/10.1021/ac00097a001

[32] He H., Zhong M., Adzima B., Luebke D., Nulwala H., Matyjaszewski K.: A simple and universal gel permeation chromatography technique for precise molecular weight characterization of well-defined poly(ionic liquid)s. Journal of the American Chemical Society, **135**, 4227–4230 (2013). https://doi.org/10.1021/ja4012645

[33] Tamagawa H., Popovic S., Taya M.: Pores and diffusion characteristics of porous gels. Polymers, **41**, 7201–7207 (2000). https://doi.org/10.1016/S0032-3861(00)00047-1

[34] Chiu Y. C., Kocagöz S., Larson J. C., Brey E. M.: Evaluation of physical and mechanical properties of porous poly (ethylene glycol)-*co*-(L-lactic acid) hydrogels during degradation. Plos One, **8**, e60728/1–e60728/11 (2013). https://doi.org/10.1371/journal.pone.0060728

[35] Kumar S. K., Douglas J. F.: Gelation in physically associating polymer solutions. Physical Review Letters, **87**, 188301 (2001). https://doi.org/10.1103/PhysRevLett.87.188301

[36] Olvera de la Cruz M., Ermoshkin A. V., Carignano M. A., Szleifer I.: Analytical theory and Monte Carlo simulations of gel formation of charged chains. Soft Matter, **5**, 629–636 (2009). https://doi.org/10.1039/B804693J

[37] Escobedo F. A., de Pablo J. J.: Molecular simulation of polymeric networks and gels: Phase behavior and swelling. Physics Reports, **318**, 85–112 (1999). https://doi.org/10.1016/S0370-1573(99)00012-5

[38] Piñeiro Redondo Y., López Quintela A., Rivas J.: MC simulation of a physical gel. Colloids and Surfaces A: Physicochemical and Engineering Aspects, **270–271**, 205–212 (2005). https://doi.org/10.1016/j.colsurfa.2005.06.004

[39] Warner Jr. H. R.: Kinetic theory and rheology of dilute suspensions of finitely extendible dumbbells. Industrial and Engineering Chemistry Fundamentals, **11**, 379–387 (1972). https://doi.org/10.1021/i160043a017

[40] Hess B., Kutzner C., van der Spoel D., Lindahl E.: GROMACS 4: Algorithms for highly efficient, load-balanced, and scalable molecular simulation. Journal of Chemical Theory and Computation, **4**, 435–447 (2008). https://doi.org/10.1021/ct700301q

[41] Swendsen R. H., Wang J-S.: Replica Monte Carlo simulation of spin-glasses. Physical Review Letters, **57**, 2607–2609 (1986). https://doi.org/10.1103/PhysRevLett.57.2607